

# *Performances of Landfill Liners under Dry and Wet Conditions*

*Saravanan Mariappan, Masashi Kamon,  
Faisal Haji Ali, Takeshi Katsumi,  
Tomoyuki Akai, Toru Inui & Masaki  
Nishimura*

**Geotechnical and Geological  
Engineering**  
An International Journal

ISSN 0960-3182

Geotech Geol Eng  
DOI 10.1007/  
s10706-011-9426-9

ISSN 0960-3182  
CODEN GGENE3

**Geotechnical  
and  
Geological  
Engineering**

AN INTERNATIONAL JOURNAL

VOLUME 24 NUMBER 2 2006

 Springer

 Springer

**Your article is protected by copyright and all rights are held exclusively by Springer Science+Business Media B.V.. This e-offprint is for personal use only and shall not be self-archived in electronic repositories. If you wish to self-archive your work, please use the accepted author's version for posting to your own website or your institution's repository. You may further deposit the accepted author's version on a funder's repository at a funder's request, provided it is not made publicly available until 12 months after publication.**

# Performances of Landfill Liners under Dry and Wet Conditions

Saravanan Mariappan · Masashi Kamon ·  
Faisal Haji Ali · Takeshi Katsumi ·  
Tomoyuki Akai · Toru Inui · Masaki Nishimura

Received: 27 April 2008 / Accepted: 25 June 2011  
© Springer Science+Business Media B.V. 2011

**Abstract** This paper addresses the study conducted on the performance of landfill liner interface parameters. Interface shear strength parameters for various combinations of 9 different lining materials were studied and presented in this paper. This comprehensive testing program covers the interfaces between: (1) soil and compacted clay liner (CCL), (2) geomembrane (HDPEs or PVC) and soil, (3) geosynthetic clay liner (GCL)/CCL and soil, (4) geomembrane and geotextile, (5) geotextile and soil, (6) geotextile and GCL/CCL, and (7) geomembrane and

GCL/CCL. The experiments were conducted for both at dry or optimum moisture condition and at saturated or wet condition. The interface performance under both conditions were compared to access the material performances. Tabulated summaries of interface test data under dry or optimum moisture condition (OMO) and saturated or wet condition are presented in the paper.

**Keywords** Landfill liner interface · Interface shear strength · Optimum moisture condition · Saturated or wet condition

---

S. Mariappan (✉) · F. H. Ali  
Department of Civil Engineering, University Malaya,  
Kuala Lumpur, Malaysia  
e-mail: vanan.nexus@gmail.com

F. H. Ali  
e-mail: fahali@gmail.com

M. Kamon · T. Katsumi · T. Akai · T. Inui ·  
M. Nishimura  
Graduate School of Global Environmental Studies, Kyoto  
University, Kyoto, Japan  
e-mail: kamon@mbox.kudpc.kyoto-u.ac.jp

T. Katsumi  
e-mail: tkatsumi@mbox.kudpc.kyoto-u.ac.jp

T. Akai  
e-mail: akai@tri.pref.osaka.jp

T. Inui  
e-mail: inui@mbox.kudpc.kyoto-u.ac.jp

M. Nishimura  
e-mail: m\_nishimura@tri.pref.osaka.jp

## 1 Introduction

The liners and closure cover system of a modern municipal solid waste (MSW) landfill are constructed with layers of material having dissimilar properties, such as compacted clay or geosynthetic clay liner, geomembrane (liquid barrier), geonet (drainage layer), geotextile (filter) and geogrid (reinforcement). While compacted clay liner or geosynthetic clay liner and geomembranes function effectively as flow barriers to leachate and infiltration, their interface peak and residual friction angles are lower than those of the soil alone. Such lower friction angle may present between geomembrane and other geosynthetics which could trigger much rapid failure during seismic loading conditions. The soil-geomembrane interface acts as a

possible plane of potential instability of the system under both static and seismic loading (Ling et al. 1997). Hence environmental geotechnical engineers are concerned about this potential instability caused by the waste containment liner system which could be fatal and also harm the environment. Hence interface tests research was conducted for both optimum moisture condition and at saturated or wet condition to understand the performance trend. The some of the test results of the finds presented in the paper were extracted from Saravanan (2006a, b and 2007).

## 2 Interface Test Material and Apparatus

The objective of this research is to study the interface shear strength of landfill liner materials. The list of interface tests conducted will dependent on the configuration and material used for landfill liner design. However, one typical liner configuration, discussed in detail in this paper is shown in Fig. 1. The research however, studied various other configuration which consists of both single and double composite liner system. The list of material used for the experiment are (1) Sand bentonite mix (100:10), (2) Silt bentonite mix (100:10), (3) Geomembrane smooth surface HDPE (Type 1), (4) Textured surface HDPE geomembrane (Type 2), (5). PVC geomembrane, (6) Needle punched Geosynthetic Clay Liner, (7) Bentonite glue Geosynthetic Clay Liner, (8) Geotextile, (9) Native Soil. As for the interface test machine, Figs. 2, 3 and 4 shows section of large scale shear box used for the research work for three different test conditions, namely (1) Case 1—Interface testing between

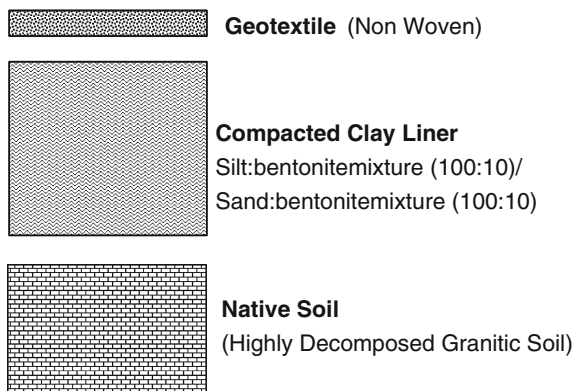


**Fig. 1** One of typical landfill liner configuration studied in the research

geosynthetic and geosynthetic, (2) Case 2—Interface testing between geosynthetic and soil, and (3) Case 3—Interface testing between soil and soil.

Bottom shear box size of  $350 \times 600$  mm and top box size of  $250 \times 500$  mm were used for the test. Larger 100 mm bottom box was used to define test failure of 15%–20% relative to lateral displacement of top box dimension. However, shearing surface contact areas were made to be similar for both top and bottom box of  $250 \times 500$  mm in size. Height adjustable bottom box base plate with spacer blocks were required to cater for variation in sample thickness and provide allowance for settlement or sample deformation during normal loading prior to shearing.

Constant shearing speed of 1 mm/min was used for test normal loads of 100, 200 and 300 kPa for the interface tests. ASTM D3080-98, ASTM D5321-02 and ASTM D6243-98 was referred for the modifications of the said shear box.

### 2.1 Physical Properties of Material Used

Physical properties of material used were investigated for all the proposed 9 test materials. Fresh soil and geosynthetic samples were used for all the tests conducted. Summary of material properties used are shown in Tables 1, 2, 3 and 4 for soil and geosynthetics, respectively.

The interface test results indicate different kind of failures at different levels of relative displacement or horizontal strain. The maximum shear stresses ranged from 1 to 15% displacement relative to sample length or top shear box size of 500 mm. In order to consistently analyze the horizontal strain and shear stresses associated with failure, the maximum shear stress was a selection of either maximum shear stress, or the maximum shear stress reached within 8% of horizontal strain.

Based on the selection criteria, the use of peak or residual interface strength is proposed to be assessed within the prescribed horizontal strain value of 8%. This is due to some of the test results have higher residual interface strength caused by horizontal strain hardening effect. Hence selection purely based on peak or residual interface strength in some cases could over or under estimate the interface resistance. Thus the selection of maximum shear stress within 8% horizontal strain was used as criteria in this research. Fig. 5

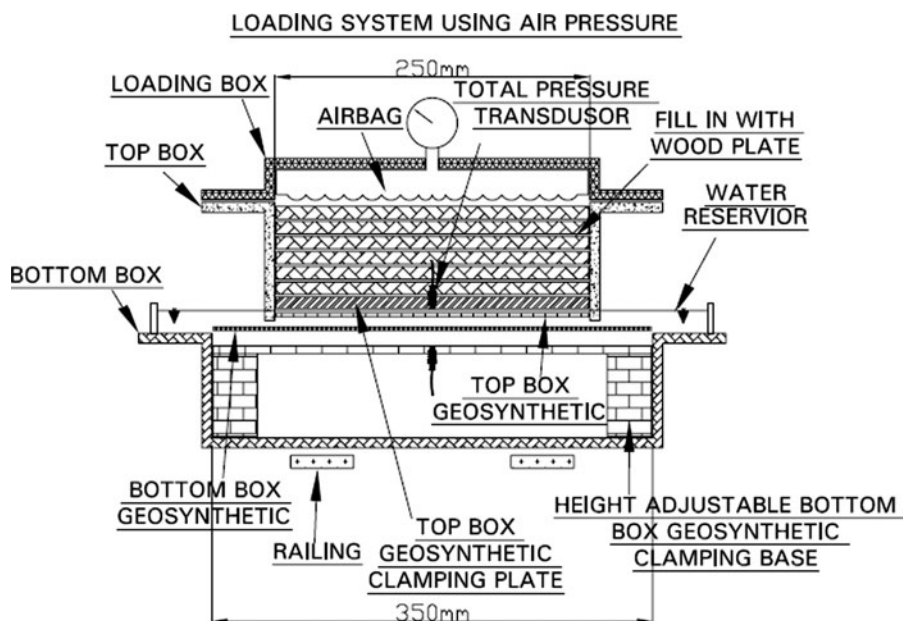
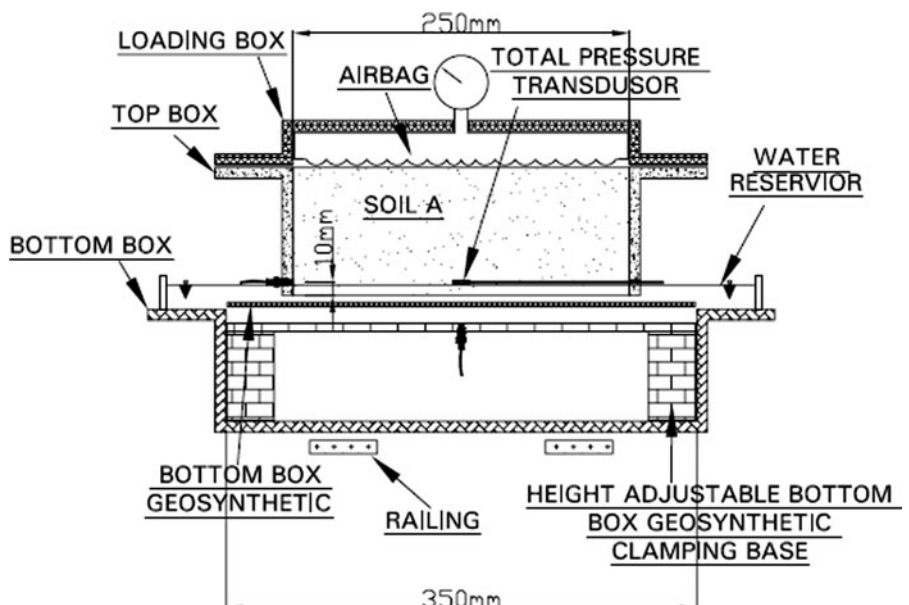


**Fig. 2** Case 1—Interface testing between geosynthetic and geosynthetic

**Fig. 3** Case 2—Interface testing between geosynthetic and soil



The unit of 8% horizontal strain was selected as criteria of landfill liner failure limit, where beyond 8% horizontal strain potential geomembrane tearing could take place leading to leachate pollution to the environment. Hence, balancing the failure criteria between geotechnically define peak and residual failure limits to failure limits which could harm the

environment due to damages created on geosynthetic material during failure were proposed. The typical details of shear stress selection method adopted is shown in Fig. 6. Horizontal strain was used to identify shear stresses in place of displacement, as the test results can be compared with tests done with various other shear box sizes as reported by Hsieh

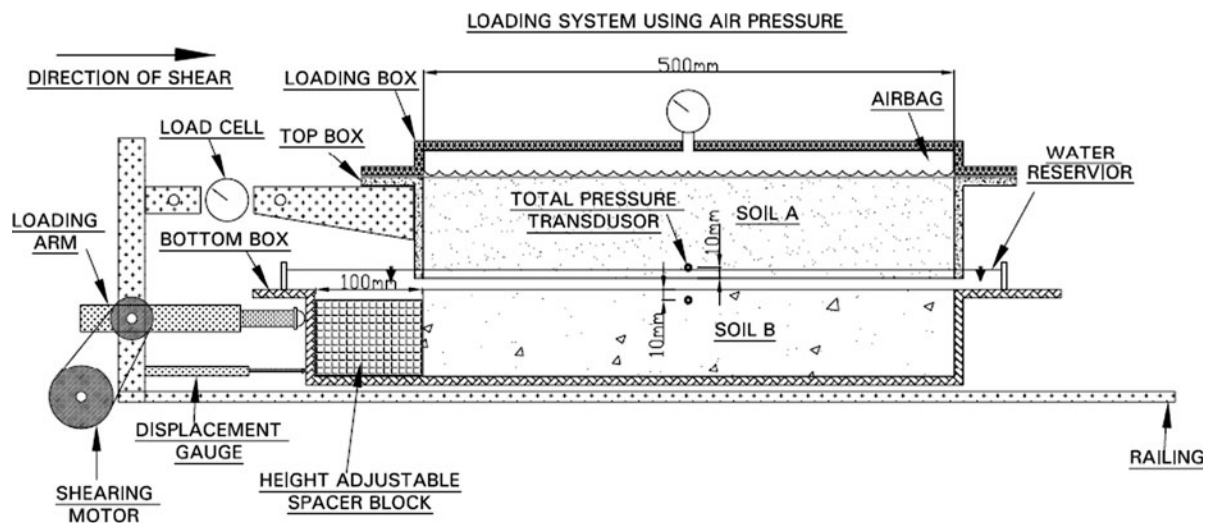


**Fig. 4** Case 3—Interface testing between soil and soil

**Table 1** Summary of the physical properties of CCLs and native base soil

Test using casagrande	Sand bentonite mixture (100:10)	Silt bentonite mixture (100:10)	Granite soil/native soil
Liquid limit, LL, $w_L$ %	47	69	—
Plastic limit, PL, $w_P$ %	23	35	—
Plasticity index, PI, $I_p$	24	34	—
Average particle density, $\rho_s$ , Mg/m <sup>3</sup>	2.60	2.64	2.59
Dry density, $\rho_d$ , Mg/m <sup>3</sup>	1.9	1.68	2.06
Optimum moisture content, MC, %	10.5	17.5	9.0
Classification as per USCS	CL/OL Organic silt or clay of low plasticity	CH/OH clay of high plasticity	Highly weathered granitic soil/SW-SM
Shear box test (internal failure)			
Total cohesion, $C_u$ , kPa	77.0	43.1	31.4
Total friction angle, $\phi^\circ$	34.3	35.8	45.5
CIU test results			
Total Cohesion, $C_u$ , kPa	5	4	5
Total friction angle, $\phi^\circ$	25	22	30
Effective cohesion, $C'_u$ , kPa	0	0	0
Effective friction angle, $\phi'^\circ$	33.5	28	35
Hydraulic conductivity, m/s	$6 \times 10^{-12}$	$8 \times 10^{-12}$	$6 \times 10^{-9}$

et al. (2003). The selected shear stresses obtained were plotted against normal stresses to compute the failure envelope. To determine the total cohesion and total interface friction angle, best-fit linear plots were developed. The shear stress intersections were set to be through either axis or positive cohesion only. List of the interface tests conducted are presented in Table 5. The interface test results obtained are

proposed to be grouped into following strength categories.

Friction ( $^\circ$ )	Cohesion (kPa)	Proposed strength
$0^\circ$ – $10^\circ$	0–10	Low
$10^\circ$ – $20^\circ$	10–20	Medium
$20^\circ$ <	20<	High

**Table 2** Summary of geosynthetic physical properties

Description	Geotextile	PVC	HDPE (Type 1 and 2)
Mass index	$\geq 1070 \text{ g/m}^2$	$\geq 1,940 \text{ g/m}^2$	$\geq 1,550 \text{ g/m}^2$
	JIS-L-1908	JIS-L-1908	JIS-L-1908
Thickness	$\geq 10.0 \text{ mm}$	$\geq 1.5 \text{ mm}$	$\geq 1.5 \text{ mm}$
	JIS-L-1908	JIS-K-6250	JIS-K-6250
Tensile strength	$\geq 160 \text{ N/cm}$ (Weft-CD)	300 N/cm for	$544 \geq 350 \text{ N/cm}$
	$\geq 80 \text{ N/cm}$ (Wrap-MD)	both Weft and Wrap	both Weft and Wrap
	JIS-L-1908		JIS-K-6251
Elongation at break	$\geq 55\%$ (Weft-CD)	320% for both	$790 \geq 560\%$ for both
	$\geq 70\%$ (Wrap-MD)	Weft and Wrap	Weft and Wrap
	JIS-L-1908		
Tear strength	$\geq 200 \text{ N}$ (Weft-MD)	N/A	$289 \geq 140 \text{ N}$
	$\geq 200 \text{ N}$ (Wrap-MD)		JIS-K-6252
	JIS-L-1096		
Penetration	$\geq 1000 \text{ N}$	N/A	$\geq 539 \text{ N}$
	ASTM D4833-88		ASTM D4833-88

**Table 3** Summary of the physical properties of bentonite-glued GCL (type 1)

Description	Properties
Finished GCL properties	
Bentonite coating (ASTM D5993)	$\geq 3.66 \text{ kg/m}^2$
Effective hydraulic conductivity (ASTM D5887/E96)	$\leq 4 \times 10^{-14} \text{ m/s}$
Bentonite moisture content (ASTM D2216)	25% typical
Geomembrane properties	
HDPE thickness (ASTM D 5994)	1.45 mm
Density (ASTM D1505)	0.94 g/cm <sup>3</sup>
Asperity height	7–10 mil
Tensile properties	
Tensile break strength (ASTM D6693)	16 N/mm
GCL tensile strength (ASTM D6768)	23 N/mm
Elongation at break (ASTM D6693)	150%
Puncture resistance (ASTM D4833)	400 N
Sodium bentonite properties	
Hydraulic flux: Bentonite, (ASTM D5887)	$\geq 1 \times 10^{-8} \text{ m}^3/\text{m}^2 \text{ s}$
Hydraulic conductivity of bentonite (ASTM D5084)	$\geq 5 \times 10^{-11} \text{ m/s}$
Free swell (ASTM D5890)	$\geq 24 \text{ ml/2 g}$
Fluid loss (ASTM D5891)	$\geq 18 \text{ ml}$

## 2.2 Hydration Methodology

In order to saturate the soil sample, (native soil and compacted clay liners) vacuum pressure was used. The compacted soil samples were placed in a vacuum chamber with maximum negative pressure between 50 and 60 kPa for 48 h. The

schematic detail of the vacuum chamber is shown in Fig. 5.

## 3 Shearing Process Methodology

Following are the test methodology adopted to perform the interface tests:

**Table 4** Summary of the physical properties of needle-punched GCL (type 2)

Description	Properties
Finished GCL properties	
Mass per unit area (EN 965)	5,000 g/m <sup>2</sup>
Thickness (EN 964-1)	6.0 mm
Max. tensile strength, md/cd <sup>a</sup> (EN ISO 10319)	12.0/12.0 kN/m
Elongation at break, md/cd <sup>a</sup> (EN ISO 10319)	10.0/6.0%
Peel strength (EN ISO 10319)	≥60 N/10 cm
Peel strength (ASTM D 6496)	≥360 N/m
Permeability/Hydraulic conductivity (DIN 18130)	$2 \times 10^{-11}$ m/s
Index flux (DIN 18130)	$5 \times 10^{-9}$ (m <sup>3</sup> /m <sup>2</sup> )/s
Geotextile layer	
Cover layer 1	
Geotextile type	Polypropylene non-woven
Mass per unit area (EN 965)	220 g/m <sup>2</sup>
Carrier layer 2	
Geotextile type	Polypropylene woven
Mass per unit area (EN 965)	110 g/m <sup>2</sup>
Bentonite layer	
Powder type	Natural sodium bentonite
Mass per unit area (EN 965)	4,670 g/m <sup>2</sup>
Swell index (ASTM D 5890)	24 ml/2 g
Fluid loss (ASTM D 5891)	≤18 ml
Water content (DIN 18121 (5 h, 105°C))	Approx. 10%

<sup>a</sup> md machine direction, cd cross machine direction

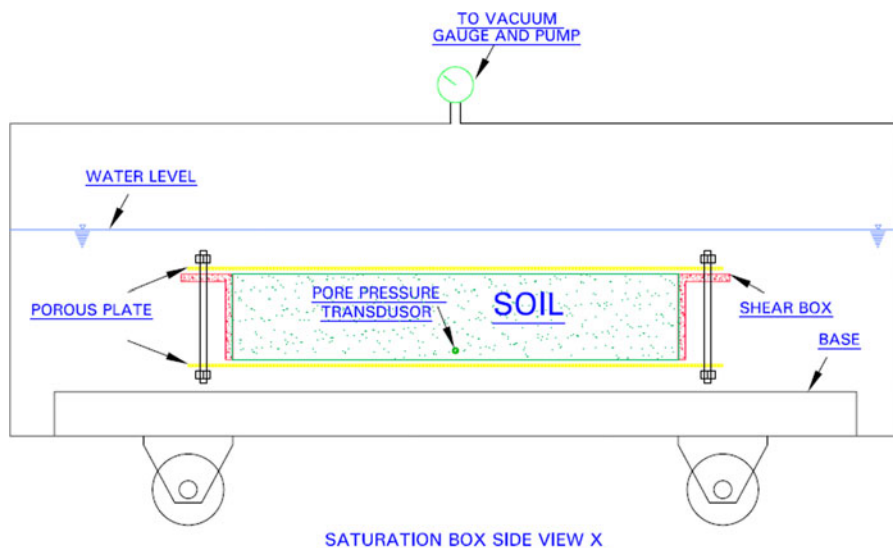


**Fig. 5** Details of saturation box or vacuum chamber used for sample Hydration

- i. The shearing machine is required to have shearing rate of 1 mm/min.
- ii. Normal loads were applied using an air bag system within a fixed frame. Due to this,
- iii. vertical displacements were restricted from taking place.
- iii. The load cell (or proving ring) used to record and monitor shearing forces had an accuracy of ± 2.5 N.

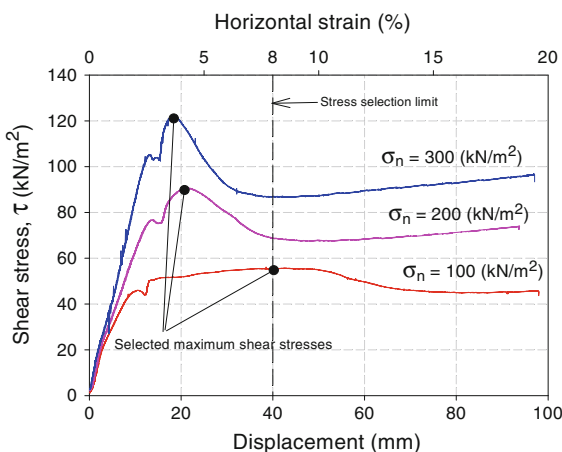


**Fig. 6** Failure stress selection criteria

- iv. The device used to measure horizontal displacement had an accuracy of  $\pm 0.02$  mm with a maximum horizontal displacement of 110 mm.
- v. Linear Variable Differential Transformers (LVDTs) were used to measure displacement.

A height adjustable bottom box base plate was introduced, along with spacer blocks, to allow for variations in sample thickness, settlement of sample deformation during normal loading prior to shearing. Due to contact area reduction during shearing, area correction method was adopted to obtain accurate shear stresses. A constant shearing speed of 1 mm/min was used along with test normal stresses of 100, 200 and 300 kPa. For tests on CCLs and decomposed granitic soil (Native soil), the sample were compacted into the shear box using an electric vibrating compacting machine with a 250  $\times$  150 mm base and mass of 5 kg. The compaction process was carefully calibrated to obtain the compaction effort required to achieve a minimum compaction dry density of 90% (compared with equivalent sample dry density obtained using 4.5 kg rammer into a CBR mould as per BS1377: Part 4: 1990) for soil samples placed in the shear box. Fresh soil was used for every individual test. The samples were compacted in the shear box in five layers, with minimum compaction time of 12 min per layer.

Before shearing the normal stresses was applied for 10–15 min for tests with GCLs, CCLs and native soil. The GCLs were considered to be under dry condition with total initial moisture condition ranging between 8 and 10%. As for CCLs and native soils, all

samples were compacted and tested at optimum moisture content (OMC). Details of samples parameters are reported in Table 1.

## 4 Test Results and Discussion

### 4.1 Geotextile Interfacing with Compacted Clay Liners (CCLs) under Dry or Optimum Moisture Condition (OMC)

The performances of silt:bentonite mixture (100:10) with geotextile had only frictional contribution without cohesion. The performance of geotextile (Test 12A) produced frictional angle of 15.2 degrees. The results are presented in Table 6 and Fig. 7 respectively. For silt:bentonite mixture (100:10) and geotextile interface the peak shear stresses were reached within horizontal strain of 4.5–5.7%. There were spots of tearing and total internal failure of geotextile took place for higher normal loads of 200 and 300 kPa. Continuous reduction in the shear stresses were observed until constant residual shear stresses were obtained beyond 10% strain. In all normal stresses there were no pre peaks, slippage or plowing effect taking place before peak stresses reached.

The interface performances of sand:bentonite mixture (100:10) with geotextile had only frictional contribution without cohesion. Geotextile (Test 19A) provided friction angle of 15.6 degrees. The test results are presented in Table 6 and Fig. 8 respectively. For sand:bentonite mixture (100:10) and geotextile interface the peak shear stresses were reached within horizontal strain of 3.1–7.3%. Continuous increment in shear stresses was observed beyond peak stresses into residual region. The geotextile was split into two during the tests. The residual shear stress behaviors were relatively similar for normal loads of 200 and 300 kPa. In all normal stresses there were no pre peaks or slippage or plowing effect taking place before peak stresses reached.

The performance of silt:bentonite mixture (100:10) and sand:bentonite mixture (100:10) were similar when interfacing with geotextile. However, the frictional contribution from the interfaces with sand:bentonite mixture (100:10) was marginally higher than that of silt:bentonite mixture (100:10). In the initial prediction, sand:bentonite mixture

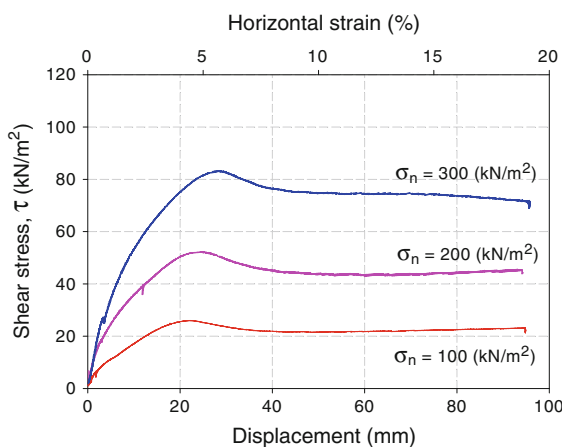
**Table 5** List of tests conducted

Interfacing material	Geotextile	Smooth HDPE (type 1)	Textured HDPE (type 2)	Rear side of PVC	Front side of PVC	Bentonite side of bentonite-glued GCL (type 1)	HDPE side of bentonite-glued GCL (type 1)	Non woven side of needle-punched GCL (type 2)	Native soil
Smooth HDPE (type 1)	Test 1A/B								
Textured HDPE (type 2)	Test 2A/B								
Rear side of PVC	Test 3A/B								
Front side of PVC	Test 3C/D								
Bentonite side of bentonite-glued GCL (type 1)	Test 4A	Test 6A	Test 8A	Test 10A	Test 10E				
HDPE side of bentonite-glued GCL (type 1)	Test 4C	Test 6C	Test 8C	Test 10C	Test 10G				
Non woven side of needle-punched GCL (type 2)	Test 5A	Test 7A	Test 9A	Test 11A	Test 11E				
Woven side of needle-punched GCL (type 2)	Test 5C	Test 7C	Test 9C	Test 11C	Test 11G				
Silt:bentonite mixture (100:10)	Test 12A/B	Test 13A/B	Test 14A/B	Test 15A/B	Test 15C/D	Test 17A	Test 17C	Test 18A	Test 18C
Sand:bentonite mixture (100:10)	Test 19A/B	Test 20A/B	Test 21A/B	Test 22A/B	Test 22C/D	Test 24A	Test 24C	Test 25A	Test 25C
Native soil	Test 26A/B	Test 27A/B	Test 28A/B	Test 29A/B	Test 29C/D				Test 23A/B

Test Type A, C, E and G—are the tests conducted under dry (optimum moisture condition), Test Type B and D—are the tests conducted under wet (saturated condition), The smooth and textured HDPE has the same surface texture on both sides of the material, hence only single side interface tests were conducted

**Table 6** Interface test results of liner configuration shown in Fig. 1 for both dry or optimum moisture condition (OMC) and wet condition

Test	Interface parameters	Cohesion (kN/m <sup>2</sup> )	Friction angle (°)
Test 12A (dry)	Silt:bentonite mixture (100:10) and geotextile	0.0	15.2
Test 12B (wet)	Silt:bentonite mixture (100:10) and geotextile	0.0	19.0
Test 19A (dry)	Sand:bentonite mixture (100:10) and geotextile	0.0	15.6
Test 19B (wet)	Sand:bentonite mixture (100:10) and geotextile	0.0	20.6
Test 16A (dry)	Native soil and silt:bentonite mixture (100:10)	10.3	28.3
Test 16B (wet)	Native soil and silt:bentonite mixture (100:10)	6.6	17.5
Test 23A (dry)	Native soil and sand:bentonite mixture (100:10)	0.0	31.0
Test 23B (wet)	Native soil and sand:bentonite mixture (100:10)	0.0	20.7

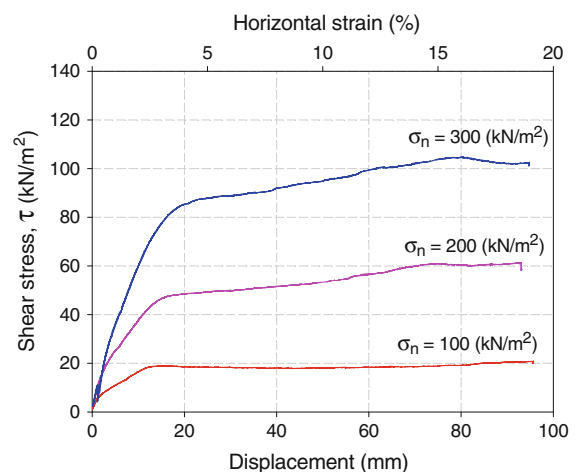
**Fig. 7** Test 12A—Interface between silt:bentonite mixture (100:10) and geotextile under dry or OMC

(100:10) was predicted to provide much higher frictional resistance as compared to silt:bentonite mixture. The test results were not as predicted due to the presence of bentonite in sand and higher damages were created on interfacing member during shearing by sand.

#### 4.2 Geotextile Interfacing with Compacted Clay Liners (CCLs) under Saturated or Wet Condition

The performances of silt:bentonite mixture (100:10) with geotextile under saturated or wet condition (Test 12B), here too only frictional contribution was exhibited without cohesion. The results are presented in Table 6 and Fig. 9.

For silt:bentonite mixture (100:10) and geotextile interface, the peak shear stresses were limited within horizontal strain of 8%. There were no spots of

**Fig. 8** Test 19A—Interface between sand:bentonite mixture (100:10) and geotextile under dry or OMC

tearing and internal failure of geotextile took place for all normal loads. Continuous increment in the shear stresses was observed for low normal stresses of 100 kPa. As for higher normal loads reduction in the shear stresses were observed beyond horizontal strain of 10–15%. In all normal stresses there were no pre peaks, slippage or plowing effect taking place before peak stresses.

As for the total stress readings from transducers installed at centre of CCL and at the perimeter wall of the shear box, it was observed that at about 3–13% horizontal strain sudden increment in shear stresses were observed for normal loads of 200 and 300 kPa. The transducer readings represent the behavior of internal shear stresses together with pore pressures which represent total stress within the CCL during interface shearing is shown in Fig. 10. This indicates

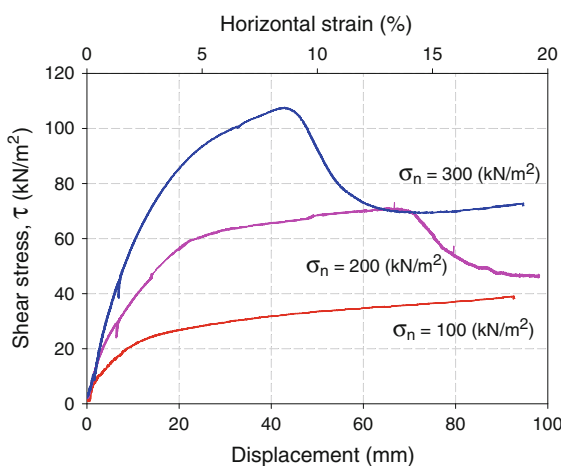


**Fig. 9** Test 12B—Silt:bentonite mixture (100:10) and geotextile interface under saturated or wet condition

the occurrences of complete failure in internal strength of CCL (silt:bentonite mixture (100:10)). This CCL failure trend is closely indicated in the interface total stress as shown in Fig. 9. As for 100 kPa normal stress the internal and perimeter total stress had no clear indication of CCL failure was reached. To record the total stress, 4 transducers were installed in the shear box at top and bottom box. Two numbers were installed at the box wall perimeter (P) and two numbers were installed at centre (I) of the interface to record the trend of total stress during interface shearing. Figure 4 shows the location of centre (I) transducer installed.

As for the performances of sand:bentonite mixture (100:10) with geotextile (Test 19B), also only frictional contribution was exhibited without cohesion. The test results are presented in Table 6 and Fig. 11.

For sand:bentonite mixture (100:10) and geotextile interface, the peak shear stresses had horizontal strain hardening for 100 kPa normal loads and horizontal strain softening for 200 and 300 kPa. Elongation of geotextile was observed, which could have caused the horizontal strain softening effect. No damage on geotextile was observed.

As for the total stress readings at centre of CCL and at the perimeter wall it was observed that at all normal stresses, the total stress reading had irregular trend during the increment in shear stresses. However, the internal total stress was observed to taper when horizontal strain softening effect was observed

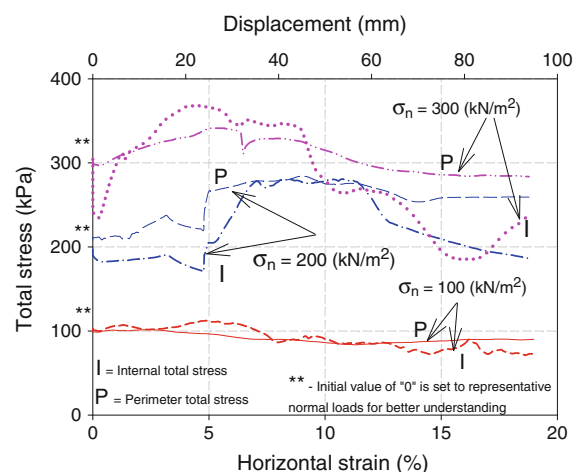


**Fig. 10** Test 12B—Silt:bentonite mixture (100:10) and geotextile total stress plot during shearing under saturated or wet condition

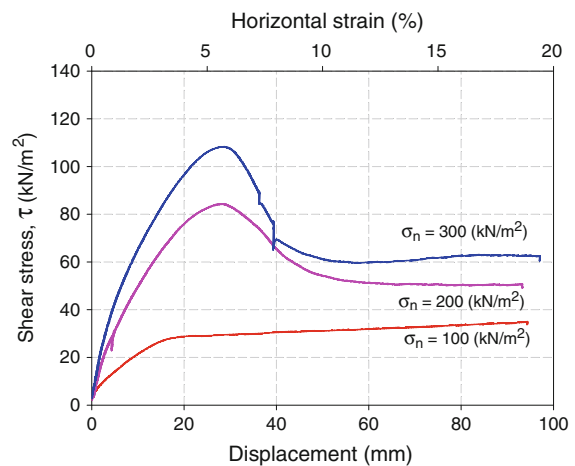


**Fig. 11** Test 19B—Interface between sand:bentonite mixture (100:10) and geotextile interface under saturated or wet condition

in the interface shear stresses (200 and 300 kPa internal total stress). As for 100 kPa normal load the internal and perimeter total stresses were generally maintained constant. The total interface shear stress plot within the CCL during shearing is shown in Fig. 12.

The performance of silt:bentonite mixture (100:10) and sand:bentonite mixture (100:10) were similar when interfacing with geotextile under wet condition. However, the frictional contribution from the interfaces with sand:bentonite mixture (100:10)

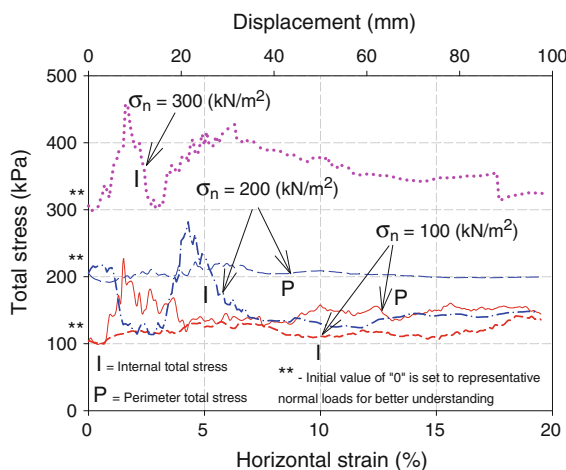


**Fig. 12** Test 19B—Sand:bentonite mixture (100:10) and geotextile total stress plot during interface shearing under saturated or wet condition

was also marginally higher than that of silt:bentonite mixture (100:10).

As for the total stress behaviour the trend of failure between internal and perimeter total stress had relatively same trend of failure for silt:bentonite mixture (100:10). However, in the case of sand:bentonite mixture (100:10) the internal total stress intend to reduce with horizontal strain, compared to perimeter total stress, which had an increasing or maintained constant trend (100 and 200 kPa). This differences could be due to failure in the sand:bentonite mixture (100:10) taking place from inside out during interface shearing. Where the center of the soil mass intend to push outwards for sand:bentonite mixture (100:10) and in the case of silt:bentonite mixture (100:10) the mass remain intact. Probability the sand:bentonite mixture (100:10) have tendency of collapsing under saturated condition as compared to silt:bentonite mixture (100:10) with the ability to remain intact.

#### 4.3 Native Soil Interfacing with Compacted Clay Liners (CCLs) under Dry or Optimum Moisture Condition (OMC)

Interface between native soil and CCLs were covered in wide range of friction angles with cohesion and frictional contribution from silt:bentonite mixture (100:10). Details of the test results are presented in Table 6 and Figs 13 and 14.

Interface between native soil and silt:bentonite mixture (100:10) (Fig. 13, Test 16A), the peak forces were reached within horizontal strain of 7.8–8.0%. Constant residual shear stresses were observed in the residual region for all normal loads, beyond 6% horizontal strain. No plowing kind of effect was observed. Good surface contact was obtained and the failure plane intrudes or cut more into silt:bentonite mixture (100:10) as compared to native soil.

In the case of native soil and sand:bentonite mixture (100:10) the peak forces were reached within horizontal strain of 8.0% (Fig. 14, Test 23A). Constant increment in residual shear stresses were observed in the residual region. No plowing kind of effect was observed. Good surface contact was obtained and the failure plane intrude or cut more into native soil as compare to sand:bentonite mixture (100:10).

The interface properties of sand:bentonite mixture (100:10) with native soil exhibits only frictional resistance except for silt:bentonite mixture (100:10) (Test 16A).

#### 4.4 Native Soil Interfacing with Compacted Clay Liners (CCLs) under Saturated or Wet Condition

For native soil and silt:bentonite mixture (100:10) interface (Fig. 15 and Test 16B in Table 6), the peak shear stresses were limited within horizontal strain of 8%. Consolidation was done for all normal loads

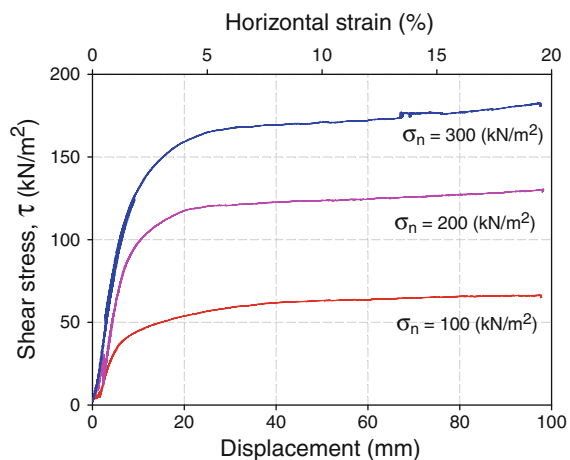


**Fig. 13** Test 16A—Interface between native soil and silt:bentonite mixture (100:10) under Dry or OMC

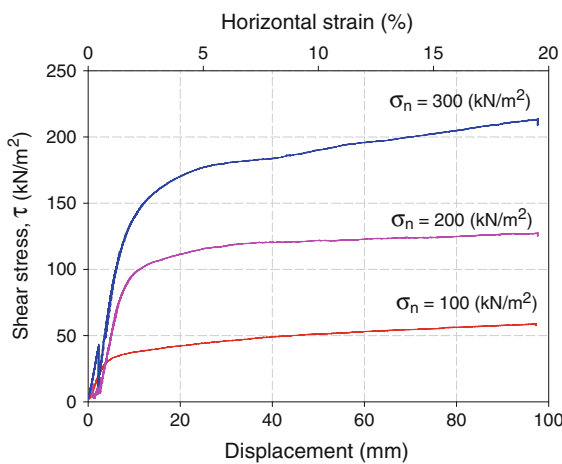


**Fig. 14** Test 23A—Interface between native soil and sand:bentonite mixture (100:10) under Dry or OMC

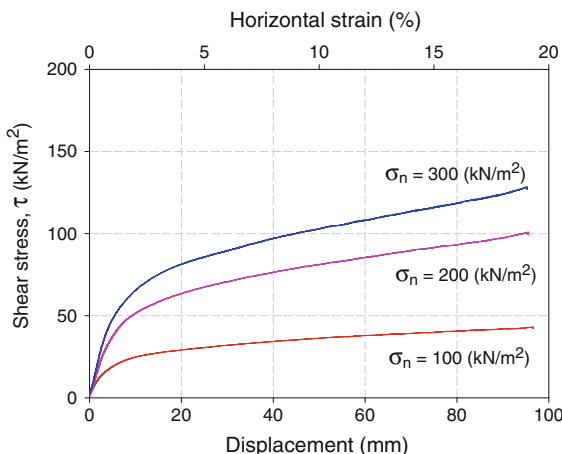


**Fig. 15** Test 16B—Interface between native soil and silt:bentonite mixture (100:10) under saturated or wet condition

prior to interface shearing to disperse the initial pore water pressure built up. The typical detail of consolidation for test normal load of 200 kPa is shown in Fig. 16a. During interface test horizontal strain hardening effect was observed for all normal loads.

As for the total stress readings at centre of native soil and silt:bentonite mixture (100:10), and at the perimeter it was observed that at all normal stresses an increment in total stress was observed except for native soil. The drop in internal total stress for native soil could be due to internal failure of native soil which pushes out the soil mass away from centre. Typical total stress plots for test normal load of 200 kPa interfaces is shown in Fig. 16b.

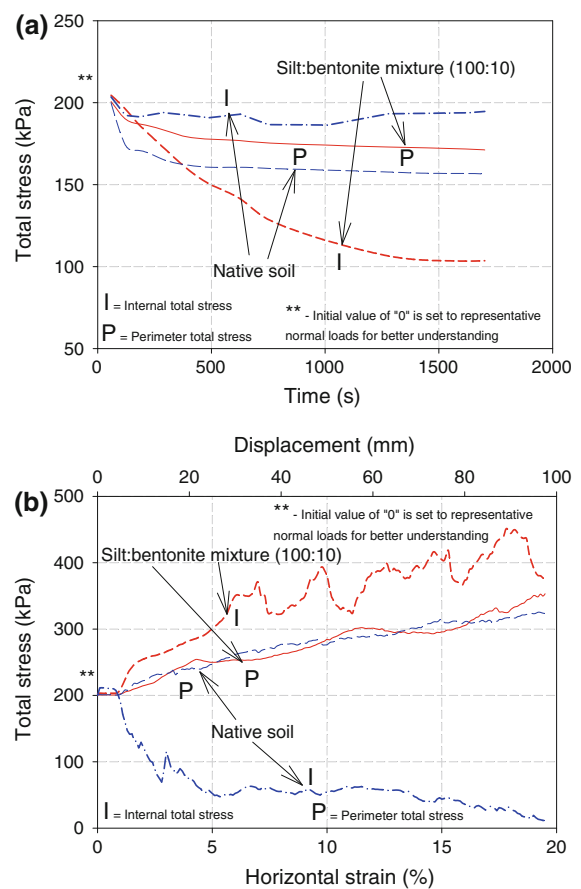


**Fig. 16** **a** Test 16B—Native soil and silt:bentonite mixture (100:10) consolidation at 200 kPa under saturated or wet condition. **b** Test 16B—Native soil and silt:bentonite mixture (100:10) total stress plot during interface shearing at 200 kPa under saturated or wet condition

For native soil and sand:bentonite mixture (100:10) interface (Fig. 17 and Test 23B in Table 1), the peak shear stresses were limited within horizontal strain of 8%. Consolidation was done for all normal loads prior to interface shearing to disperse the initial pore water pressure built up. The typical detail of consolidation for normal load of 300 kPa is shown in As for the total stress readings at centre and at the perimeter it was observed that at all normal stresses an increment in total stress was observed except for 300kpa. The drop in internal total stress for native soil and CCL could be due to internal failure of both native soil and CCL especially (both of sand and silt:bentonite mixture). Typical total stress plots for test normal load of 300 kPa interfaces are shown in Fig. 18b.

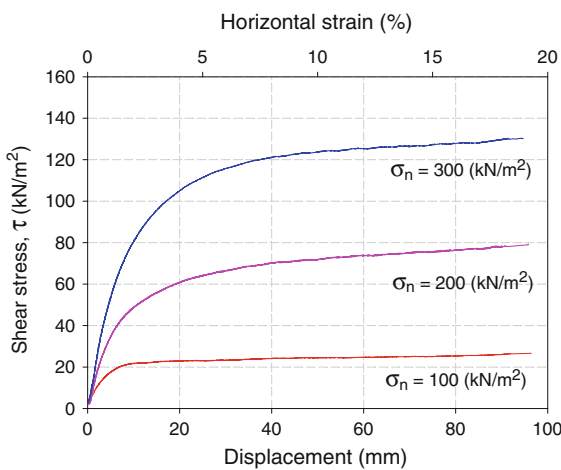


**Fig. 17** Test 23B—Interface between native soil and sand:bentonite mixture (100:10) under saturated or wet condition

Summary details of other interface test results are presented in Table 7 and Table 9 for tests conducted under saturated (wet) condition and optimum moisture condition (OMC) (dry), respectively. Similarly the summary of stress and horizontal strain relationship for the tests conducted under saturated (wet) condition and optimum moisture condition (OMC) (dry) is shown in Table 8 and 10 respectively. Various other interface test configuration tested are listed in Table 5.

The research program covers the interfaces between: (1) Soil and Compacted Clay Liner (CCL), (2) Geomembrane (HDPEs or PVC) and soil, (3) Geosynthetic Clay Liner (GCL)/CCL and soil, (4) Geomembrane and geotextile, (5) Geotextile and soil, (6) Geotextile and GCL/CCL, and (7) Geomembrane and GCL/CCL. The experiments were conducted for both optimum moisture condition (OMC) (dry) and at saturated or wet condition.

## 5 Discussion and Conclusions

a. Geotextile interfacing with geomembranes (HDPE Type 1, HDPE Type 2 and PVC) the interface test results had very little different between optimum moisture condition (OMC) and saturated condition. Only in the case of front side of PVC geomembrane higher frictional resistance was observed about 30% higher.

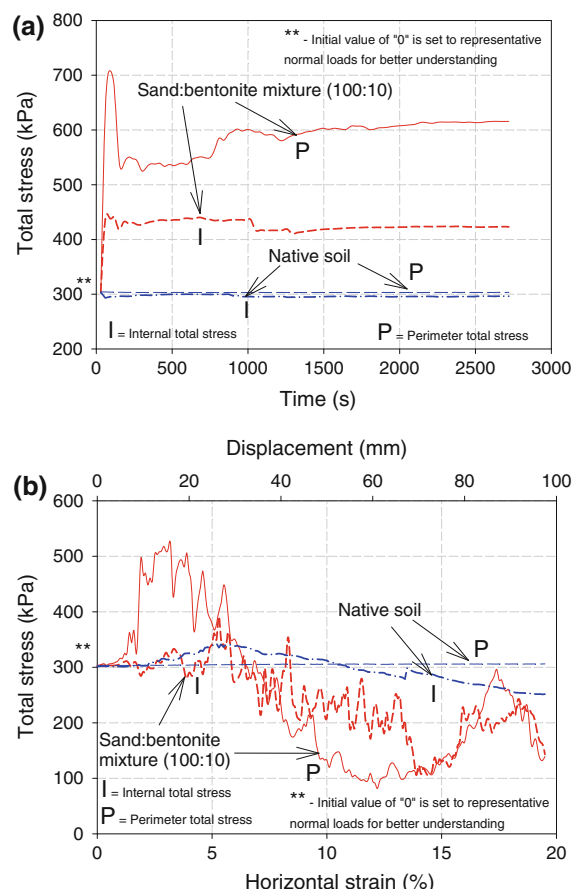


**Fig. 18** **a** Test 23B—Native soil and sand:bentonite mixture (100:10) consolidation at 300 kPa under saturated or wet condition. **b** Test 23B—Native soil and sand:bentonite mixture (100:10) total stress plot during interface shearing at 300 kPa under saturated or wet condition

- Silt:bentonite mixture (100:10) interfacing with geotextile and geomembrane (HDPE Type 1, HDPE Type 2 and PVC) the interface test results was lower for saturated condition compared to OMC of about 62–195%. The HDPEs had frictional resistant lowered by 165–195% and PVC geomembrane by 62–88%. However, 20% increment in frictional resistance was observed in the case of geotextile.
- Sand:bentonite mixture (100:10) interfacing with geotextile and geomembrane the interface test results were similar to those of with silt:bentonite mixture (100:10). The saturated interfaces were lower for geomembrane compared to geotextile. The geomembrane had the frictional resistance lowered by 125–463%.

**Table 7** Summary of interface peak shear strength under wet or saturated condition

Interfacing material c: cohesion in kN/m <sup>2</sup> $\phi$ : frictional angle in degree.	Geotextile		Smooth HDPE (type 1) geomembrane		Textured HDPE (type 2) geomembrane		Rear side of PVC geomembrane		Front side of PVC geomembrane		Native soil	
	c	$\phi$	c	$\phi$	c	$\phi$	c	$\phi$	c	$\phi$	c	$\phi$
Smooth HDPE (type 1) geomembrane	0.0	7.3										
Textured HDPE (type 2) geomembrane	8.7	20.6										
Rear side of PVC geomembrane	6.1	18.2										
Front side of PVC geomembrane	0.0	22.3										
Silt:bentonite mixture (100:10)	0.0	19.0	0.0	5.2	0.0	9.1	0.0	13.7	2.4	10.5	6.6	17.5
Sand:bentonite mixture (100:10)	0.0	20.6	0.0	6.1	0.0	10.9	0.0	3.5	0.0	6.5	0.0	20.7
Native soil	9.9	18.6	0.0	19.8	26.8	15.2	9.3	17.5	0.0	19.8		

**Table 8** Summary of stress and horizontal strain relationship for the interface combinations tested under saturated condition or wet condition

Interfacing material	Geotextile	Smooth HDPE (Type 1) geomembrane	Textured HDPE (Type 2) geomembrane	Rear side of PVC geomembrane	Front side of PVC geomembrane	Native soil
Smooth HDPE (type 1) geomembrane	SH-F13	1.2–7.8 <sup>a</sup>				
Textured HDPE (type 2) geomembrane	SS-F35	3.2–4.2 <sup>a</sup>				
Rear side of PVC geomembrane	SH-F48B	7.8–8.0B <sup>a</sup>				
Front side of PVC geomembrane	SH-F48B	5.5–8.0B <sup>a</sup>				
Silt:bentonite mixture (100:10)	SC F48B	SH F48B	SH F48B	SH F48B	SH F48B	SH F48B
	8.0B <sup>a</sup>	8.0B <sup>a</sup>	8.0B <sup>a</sup>	8.0B <sup>a</sup>	8.0B <sup>a</sup>	8.0B <sup>a</sup>
Sand:bentonite mixture (100:10)	SC F48B	SH F48B	SH F48B	SH F48B	SH F48B	SH F48B
	5.7–8.0B <sup>a</sup>	8.0B <sup>a</sup>	3.1–8.0B <sup>a</sup>	7.8–8.0B <sup>a</sup>	8.0B <sup>a</sup>	8.0B <sup>a</sup>
Native soil	SC-F48B	SH-F13	SH-F48B	SC-F35	SC-F35	
	5.0–8.0B <sup>a</sup>	1.5–3.8 <sup>a</sup>	7.9–8.0B <sup>a</sup>	3.8–4.7 <sup>a</sup>	2.2–4.5 <sup>a</sup>	

SH: Horizontal strain hardening behavior for all normal stress levels tested, SS: Horizontal strain softening behavior for all normal stress levels tested, SC: Stress and horizontal strain behavior depends upon the normal stress levels. Horizontal strain hardening for low normal stress and horizontal strain softening for high normal stress, F13, F35, or F46: Failure occurred within the 1–3%, 3–5%, or 4–6% of horizontal strain respectively, F48B: Failure occurred within the 4–8% horizontal strain or beyond

<sup>a</sup> Horizontal strain at peak shear stress

The HDPEs had frictional resistant lowered by 125% and PVC geomembrane by 160–463%. However, 25% increment in frictional resistance was observed in the case of geotextile.

d. Interface of native soil with geotextile, geomembrane and CCLs compared with optimum

moisture condition (OMC) and saturated condition had following findings:

- with geotextile—4% higher frictional resistant.
- with smooth HDPE (Type 1) geomembrane—21% higher frictional resistant.
- with textured HDPE (Type 2) geomembrane—50% lower frictional resistant.

**Table 9** Summary of interface peak shear strength for the interface combinations tested under dry or optimum moisture condition (OMC) (Saravanan 2007)

Interfacing material c: cohesion in kN/m <sup>2</sup> $\phi$ : frictional angle in degree.	Geotextile	Smooth HDPE (type 1)	Textured HDPE (type 2)	Rear side of PVC geomembrane	Front side of PVC geomembrane	Bentonite side of bentonite- glued GCL (type 1)	HDPE side of bentonite- glued GCL (type 1)	Non woven side of needle- punched GCL (type 2)	Native soil
	c	$\phi$	c	$\phi$	c	$\phi$	c	$\phi$	c
Smooth HDPE (type 1) geomembrane	0.0	7.6							
Textured HDPE (type 2) geomembrane	3.0	21.0							
Rear side of PVC geomembrane	11.3	18.6							
Front side of PVC geomembrane	26.3	16.9							
Bentonite side of bentonite- glued GCL (type 1)	11.5	17.2	0.0	9.0	28.9	18.7	19.0	17.7	0.0
HDPE side of bentonite-glued GCL (type 1)	0.0	21.8	2.2	8.9	0.0	19.8	11.8	20.0	0.0
Non woven side of needle- punched GCL (type 2)	1.3	15.0	2.3	7.7	10.4	25.4	17.0	15.2	11.0
Woven side of needle-punched GCL (type 2)	10.6	14.7	2.4	9.2	2.5	22.9	14.4	18.0	22.8
Silt:bentonite mixture (100:10)	0.0	15.2	0.0	15.3	0.0	24.1	0.0	22.2	0.0
Sand:bentonite mixture (100:10)	0.0	15.6	0.0	13.7	0.0	24.5	0.0	19.7	0.0
Native soil	0.0	17.8	0.0	15.6	0.0	23.0	0.0	18.7	0.0

**Table 10** Summary of stress and horizontal strain relationship for the interface combinations tested under dry or optimum moisture condition (OMC) (Saravanan 2007)

Interfacing material	Geotextile	Smooth HDPE (type 1) geomembrane	Textured HDPE (type 2) geomembrane	Rear side of PVC geomembrane	Front side of PVC geomembrane	Bentonite side of bentonite - glued GCL (type 1)	HDPE side of bentonite - glued GCL (type 1)	Non woven side of needle-punched GCL (type 2)	Woven side of needle-punched GCL (type 2)	Native soil
Smooth HDPE (type 1) geomembrane	SH-F13	0.7–0.9 <sup>a</sup>								
Textured HDPE (type 2) geomembrane	SS-F35	3.7–4.9 <sup>a</sup>								
Rear side of PVC geomembrane	SH-F48B	5.1–8.0B <sup>a</sup>								
Front side of PVC geomembrane	SC-F48B	5.6–8.0B <sup>a</sup>								
Bentonite side of bentonite-glued GCL (type 1)	SS-F35	SH-F13 4.1–4.8 <sup>a</sup>	1.1–1.8 <sup>a</sup>	SC-F35 3.0–3.8 <sup>a</sup>	SH-F48B 5.6–8.0B <sup>a</sup>	SH-F13 1.6–8.0B <sup>a</sup>	SH-F13 1.6–8.0B <sup>a</sup>			
HDPE side of bentonite-glued GCL (type 1)	SS-F35	SH-F48B 4.2–4.5 <sup>a</sup>	7.8–8.0B <sup>a</sup>	SH-F35 3.4–4.1 <sup>a</sup>	SH-F13 1.0–1.4 <sup>*</sup>	SH-F13 1.7–2.0 <sup>a</sup>	SH-F13 1.7–2.0 <sup>a</sup>			
Non woven side of needle-punched GCL (type 2)	SS-F35	SH-F13 3.1–4.0 <sup>a</sup>	1.1–1.6 <sup>a</sup>	SS-F35 3.1–4.5 <sup>a</sup>	SH-F46 4.6–6.1 <sup>*</sup>	SH-F48 4.4–7.8 <sup>a</sup>	SH-F48 4.4–7.8 <sup>a</sup>			
Woven side of needle-punched GCL (type 2)	SH-F35	SH-F13 3.9–4.4 <sup>a</sup>	0.9–1.6 <sup>a</sup>	SS-F35 2.7–4.1 <sup>a</sup>	SC-F48 5.1–8.0 <sup>*</sup>	SC-F48B 4.2–8.0B <sup>a</sup>	SC-F48B 5.7–8.0B <sup>a</sup>	SC-F48 5.8–7.2 <sup>a</sup>	SC-F48 5.5–7.8 <sup>a</sup>	SH-F48B 7.8–8.0B <sup>*</sup>
Silt:bentonite mixture (100:10)	SH-F46	SH-F13 4.5–5.7 <sup>a</sup>	1.2–1.9 <sup>a</sup>	SC-F48B 5.0–8.0B <sup>a</sup>	SC-F48 3.3–7.9 <sup>a</sup>	SH-F46 4.4–6.0 <sup>a</sup>	SC-F48B 5.7–8.0B <sup>a</sup>	SC-F48 5.8–7.2 <sup>a</sup>	SC-F48 5.5–7.8 <sup>a</sup>	SH-F48B 7.8–8.0B <sup>*</sup>
Sand:bentonite mixture (100:10)	SH-F48	SH-F13 3.1–7.3 <sup>a</sup>	0.8–1.9 <sup>a</sup>	SH-F48B 8.0B <sup>a</sup>	SC-F48B 5.8–8.0B <sup>a</sup>	SH-F13 3.8–8.0B <sup>a</sup>	SC-F48B 5.6–8.0B <sup>a</sup>	SC-F48B 4.0–8.0B <sup>a</sup>	SC-F48B 6.7–8.0B <sup>a</sup>	SH-F48B 8.0B <sup>a</sup>

**Table 10** continued

Interfacing material	Geotextile	Smooth HDPE (type 1) geomembrane	Textured HDPE (type 2) geomembrane	Rear side of PVC geomembrane	Front side of PVC geomembrane	Bentonite side of bentonite-glued GCL (type 1)	HDPE side of bentonite-glued GCL (type 1)	Non woven side of needle-punched GCL (type 2)	Woven side of needle-punched GCL (type 2)	Native soil
Native soil	SC-F48 4.2–7.9 <sup>a</sup>	SH-F13 1.1–2.8 <sup>a</sup>	SH-F48B 7.0–8.0B <sup>a</sup>	SC-F35 2.8–4.7 <sup>a</sup>	SC-F35 1.7–3.0 <sup>a</sup>					

SH: Horizontal strain hardening behavior for all normal stress levels tested, SS: Horizontal strain softening behavior for all normal stress levels tested, SC: Stress and horizontal strain behavior depends upon the normal stress levels. Horizontal strain hardening for low normal stress and softening for high normal stress, F13, F35, or F48; Failure occurred within the 1–3%, 3–5%, or 4–6% of horizontal strain respectively, F48B: Failure occurred within the 4–8% horizontal strain or beyond

<sup>a</sup> Horizontal strain at peak shear stress

- PVC geomembrane of both side—2–7% lower frictional resistant.
- Both CCLs—50–60% lower frictional resistant.

from the finding geotextile and smooth HDPE (Type 1) geomembrane had higher frictional resistance compared to textured HDPE (Type 2) geomembrane and PVC geomembrane. In the case of HDPEs, the frictional resistance of textured HDPE (Type 2) geomembrane had significant drop from 23.0 degrees at OMC to 15.2 degrees at saturated condition, which is almost similar to the frictional resistance of smooth HDPE (Type 1) geomembrane under OMC of 15.6 degree. As for PVC geomembrane only a drop of 2–7% was observed in frictional resistant. However, in the case of CCL 50–60% drop in interface frictional resistance was observed.

To conclude in all cases geotextile had higher frictional resistance under saturated (wet) condition compared with OMC (Dry). Only with the interface between geotextile and both sides of PVC geomembrane had a significant drop of 30% in frictional resistance was observed between optimum moisture condition (OMC) (dry) and saturated (wet) condition. The results presented in Table 7 and 9, shows interface test results of various configuration. Table 8 and 10 shown the stress and horizontal strain relationship of the interface test, indicating the failure trend during interface failure.

**Acknowledgments** The authors wish to extend special thanks to: all the individuals and institutions involved directly and indirectly by providing financial and material support for this research work, especially Japan Society for the Promotion of Science (JSPS) for their financial support.

## References

- ASTM D3080 (1998) Standard test method for direct shear test of soils under consolidated drained conditions. ASTM International, West Conshohocken, PA
- ASTM D5321 (2002) Standard test method for determining the coefficient of soil and geosynthetic or geosynthetic and geosynthetic friction by the direct shear method. ASTM International, West Conshohocken, PA
- ASTM D6243 (1998) Standard test method for determining the internal and interface shear resistance of geosynthetic clay liner by the direct shear method. ASTM International, West Conshohocken, PA
- Hsieh C, Hsieh MW (2003) Load plate rigidity and scale effects on the frictional behaviour of sand/geomembrane interfaces. *Geotext Geomembr* 21:25–47

- Ling HI Leshchinsky D (1997) Seismic stability and permanent displacement of landfill cover systems. *J Geotech Geo-environmental Eng* 123(2):113–122
- Saravanan M Kamon M Faisal HA Katsumi T Akai T Inui T Matsumoto A (2006a) Landfill stability assessment using interface parameters, In: Proceeding of the 6th Japan-Korea-France joint seminar on geoenvironmental engineering, Kyoto, Japan, pp 137–146
- Saravanan M Kamon M Faisal HA Katsumi T Akai T Inui T, Matsumoto A (2006b) Interface shear stress parameter evaluation for landfill liner using modified large scale shear box. In: Kuwano J, Koseki J (eds.) Proceedings of the 8th international conference on geosynthetics, pp 265–271
- Saravanan M (2007) Interface shear strength of composite landfill liner. PhD Thesis submitted to Kyoto University under Graduate School of Global Environmental Studies